Primljen / Received: 15.12.2014.
Ispravljen / Corrected: 11.2.2015.
Prihvaćen / Accepted: 20.2.2015.
Dostupno online / Available online: 10.5.2015.

Capacity degradation and crack pattern development in a multi-storey unreinforced masonry building

Authors:

Assist.Prof. Naida Ademović, PhD. CE
University of Sarajevo
Faculty of Civil Engineering
naidadem@yahoo.com

Prof. Mustafa Hrasnica, PhD. CE
University of Sarajevo
Faculty of Civil Engineering
hrasnica@bih.net.ba

Subject review

Naida Ademović, Mustafa Hrasnica

Capacity degradation and crack pattern development in a multi-storey unreinforced masonry building

A seismic assessment of a typical unreinforced masonry residential building without tie beams is presented in the paper. The numerical analysis was conducted according to the finite-element method using experimental data on the quality of the masonry constitutive elements and reinforced concrete. The computation was made using the nonlinear static pushover analysis and nonlinear dynamic time history analysis. The crack development pattern was compared for the procedures, as well as parts of the hysteresis curves.

Key words:
unreinforced masonry building, nonlinear material behaviour, pushover analysis, nonlinear time history analysis, crack development

Pregledni rad

Naida Ademović, Mustafa Hrasnica

Degradacija kapaciteta i razvoj pukotina višekatne nearmirane zidane građevine

U radu je prikazana seizmička procjena tipične višekatne nearmirane zidane stambene zgrade bez serklaža. Numerička analiza provedena je pomoću metode konačnih elemenata koristeći eksperimentalne podatke o kvaliteti materijala konstitutivnih elemenata ziđa i armiranog betona. Proračun je proveden nelinearnom statičkom metodom postupnog guranja (eng. Pushover Analysis) i nelinearnom dinamičkom metodom u vremenu (eng. Time History Analysis). Uspoređen je razvoj pukotina dobivenih primjenom obje proračunske metode kao i dijelovi histereznih krivulja.

Ključne riječi:
nearmirana zidana konstrukcija, nelinearno ponašanje materijala, metoda postupnog guranja, nelinearna dinamička metoda u vremenu, razvoj pukotina

Übersichtsarbeit

Naida Ademović, Mustafa Hrasnica

Kapazitätsdegradation und Rissbildung eines mehrstöckigen unbewehrten Mauerwerksgebäudes

In dieser Arbeit wird die seismische Beurteilung eines typischen mehrstöckigen unbewehrten Mauerwerksgebäudes ohne Ringanker dargestellt. Numerische Analysen wurden mittels der FEM durchgeführt und beruhten auf experimentellen Daten zu den Materialeigenschaften der Bestandteile von Mauerwerk und Stahlbeton. Zur Berechnung wurde sowohl die nichtlineare statische Pushover-Methode, als auch die nichtlineare dynamische Zeitverlaufsmethode angewandt. Für beide Berechnungsmethoden wurden der Verlauf der Rissbildung und die Hysteresekurven verglichen.

Schlüsselwörter:
unbewehrtes Mauerwerksgebäude, nichtlineares Materialverhalten, Pushover-Methode, nichtlineare dynamische Zeitverlaufsmethode, Rissbildung

1. Introduction

The existing buildings in Bosnia and Herzegovina are mostly built as masonry buildings. The traditional art of construction involved masonry buildings, built as unreinforced masonry (URM) with wooden floors [1, 2]. Half-prefabricated reinforced concrete floors were first used during the mid-1930s and this practice resumed once again after World War II. Most of these buildings had up to five storeys, but were built without vertical reinforced concrete (RC) confining elements. The seismic resistance was provided by structural walls laid in two main orthogonal directions, whereas functional demands were met by a smaller number of walls in longitudinal direction.

Several strong earthquakes that occurred over the past few decades underscore the importance of seismic vulnerability assessment, including evaluation of possible strengthening and retrofitting measures.

One of the most devastating earthquakes that struck the Balkan region was the 1963 Skopje (Macedonia) earthquake. The magnitude of the earthquake was 6.1 on the Richter's scale, and the MSC intensity was IX. The destroyed residential masonry building shown in Figure 1 is representative of typical structures built between 1950 and 1960. Although similar-type structures were exposed to earthquake actions in Slovenia, the largest and the most significant damage to this type of structures was observed during the Skopje earthquake in 1963.

It is only after the Skopje earthquake that the first seismic codes were published, and vertical confining RC elements were introduced into the masonry building practice. Presently, confining masonry is a common feature of masonry structures. The structure chosen for the analysis is similar, by structural type, to the one destroyed during the Skopje earthquake (Figure 1). This was a way of building that was traditionally applied throughout the entire Western Balkans region.

Figure 1. Destroyed residential masonry building (five storeys) [3]

According to EMS-98, structures are classified with regard to their seismic vulnerability [4]. Vulnerability classes range from A to F and this has enabled the use of one scheme with different kinds of buildings, and the variety of their ranges of vulnerability. This scale indicates how differences in the way buildings respond to earthquake actions are expressed. Buildings are classified according to their structural type, seismic intensity, and expected grade of damage [2]. Damage grades from 1 to 5, defined in the EMS-98, ideally represent a linear increase in the strength of shaking. If the structure is defined as belonging to damage grade 1, this means that it has negligible to slight damage of non-structural elements, and that it exhibits no structural damage. At the other extreme, the grade 5 illustrates a very heavy structural damage described as destruction.

This building with concrete floors belongs to the unconfined masonry, and is less than 60 years old. For the 7th degree of seismic intensity (corresponding to the Sarajevo region where the building is located), a moderate to heavy damage (grades 3 to 4) can be expected [2].

2. Modelling of masonry structures

The modelling of the existing masonry structures with regard to seismic action is a very complex task because of constitutive characteristics of the structural material, and its non-linear behaviour when subjected to strong ground motion. The numerical representation of masonry generally involves two approaches: the focus can be placed on the micro-modelling of individual components, brick unit, mortar, and the unit to mortar interface, or the macro-modelling of masonry, where units, mortar, and unit-mortar interface, are smeared out in a homogeneous continuum [5]. The micro-modelling approach is required when better understanding of local behaviour of masonry structures is needed. Consequently, this procedure is applicable for structural details and small elements (masonry prisms, wallets, etc.). As an entire structure was to be modelled, the macro-modelling and homogenization study was considered to be more adequate. Material properties necessary for numerical modelling are explained in the following sections.

2.1. Material properties

2.1.1. Compressive strength of masonry

According to Eurocode 6 [6], the characteristic compressive strength of unreinforced masonry made using general purpose mortar, with longitudinal mortar joints considered as filled, taking into account the δ-coefficient (shape coefficient), is obtained by the equation (1):

$$f_k = K \cdot f_b^{0.70} \cdot f_m^{0.30} \quad (1)$$

where:

f_k - the characteristic compressive strength of the masonry in N/mm^2

K - the constant depending on the type of masonry unit and mortar
f_b - the normalized mean compressive strength of the units, in the direction of the applied force in N/mm²
f_m - the compressive strength of the mortar in N/mm².

2.1.2. Modulus of elasticity

If there are no experimental data, Eurocode 6 [6] recommends taking the modulus of elasticity equal to (2):

$$E = 1000 \cdot f_k \text{ [MPa]} \quad (2)$$

or as indicated in equation (3), Pauley [7] recommends a value of

$$E = 750 \cdot f_k \text{ [MPa]} \quad (3)$$

2.1.3. Compressive and tensile fracture energy

According to Lourenço [8], and based upon the Model Code 90 [9] for concrete, the tensile fracture energy can be calculated using the expression (4):

$$G_f = 0{,}025 \cdot (2 \cdot f_t)^{0.7} \text{ [N/mm]} \quad (4)$$

where:
f_t - the tensile strength of the masonry in N/mm²

assuming that the tensile strength to compressive strength ratio is 5 %. The ductility index is defined by the ratio (5):

$$d = \frac{G_f}{f_t} \quad (5)$$

and, for brick, it has a recommended value of 0.029 mm [10]. The determination of the compressive fracture energy is also based on the Model Code 90 [9] for the peak strain of 0.2 %, as shown in Figure 2.

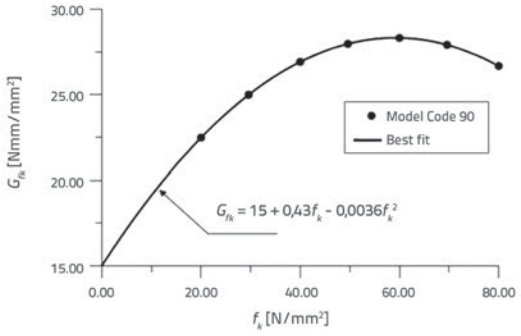

Figure 2. Compressive fracture energy according to Model *Code 90* [9]

The applicability of this curve varies from 12 to 80 N/mm², and it is calculated from the equation (6):

$$G_{fk} = 15 + 0{,}43 \cdot f_k - 0{,}036 \cdot f_k^2 \quad \text{[N/mm]} \quad (6)$$

whereas the values of d = 1.6 mm and d = 0.33 mm are recommended for $f_k < 12$ N/mm² and $f_k > 80$ N/mm², respectively [10]. Additional data can be found in [11-13].

2.1.4. Non-linear behaviour

A parabolic stress-strain relation for compression, based on the Hill-type yield criterion, was chosen for nonlinear behaviour of masonry, with no lateral confinement and no lateral crack reduction. The tension path, based on the Rankine-type yield criterion, was described by an exponential tension-softening diagram. The post-cracked shear behaviour was defined by taking into account the retention factor of its linear behaviour, the shear retention factor, β = 0.01. More details are provided in [11-13]. This material nonlinearity is presented in Figure 3.

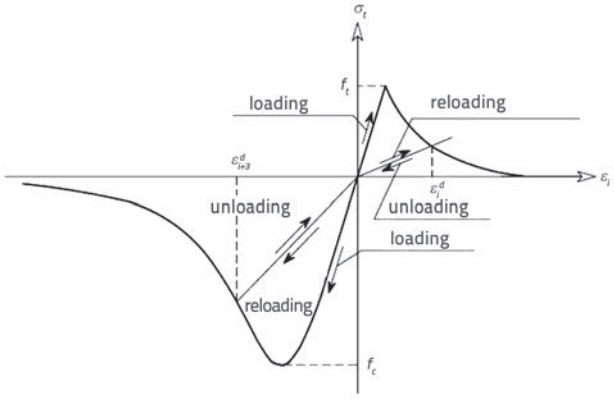

Figure 3. Nonlinear behaviour of masonry [14]

3. Case study

3.1. Description of structure

The typical residential masonry building analysed in the paper is located in Sarajevo, in the part of the city called Grbavica (Figure 4).

Figure 4. Analysed building built in 1957

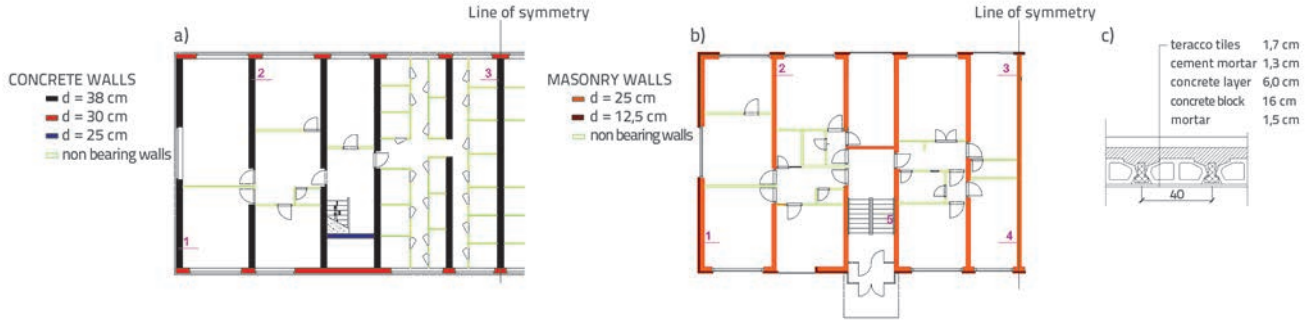

Figure 5. a) Floor plan of the studied building; b) plan view of the basement; c) "Herbst" elements

The plan view given in Figure 5 shows the layout of the structure with the load bearing walls mainly in Y direction. The structure was designed and built in 1957. It is interesting to note that, at that time, no seismic codes were applied in this region. It is only after the severe 1963 Skopje earthquake that seismic regulations were introduced and enforced in the region.

3.2. Geometry and materials

In plan, the structure measures 38.0 m by 13.0 m, and is made of 7 levels (basement + ground floor + 5 storeys). The structure is composed of load bearing walls mainly in transverse direction (Y direction) as shown in Figure 5.a, with slabs made of semi-prefabricated elements. The longitudinal façade walls (X direction) are weakened with a large number of openings (Figure 4), while in transverse direction the outer walls have just one opening on each floor. Transverse (inner) walls have door openings, in the area from 2.3 m^2 to 6.9 m^2. The total area of the outer-wall openings on the ground floor in X direction amounts to 19.8 %, while in Y direction it equals to 8.6 % only. A significant percentage of openings can be noted in longitudinal walls, where the openings amount to 46 % of the wall area. So, the lateral resistance in longitudinal direction is largely inferior compared to the lateral resistance in perpendicular (transverse) direction.

The inner load bearing walls (Y-direction) are made of brick elements 0.25 m in total thickness, while the façade walls have additional hollow brick elements 0.125 m in thickness. Bricks are of standard size, 25x12x6.5 cm, and are joined together with cement mortar.

Basement walls are made of concrete. Walls in Y direction are 0.38 m in thickness, while the outer walls in X (longitudinal) direction are 0.30 m in thickness. Two inner walls are 0.25 m in thickness (Figure 5.b). The slabs are made of semi-prefabricated "Herbst" concrete hollow elements (Figure 5.c).

3.3. Visual inspection and experimental investigations

Visual inspection revealed that there were no changes regarding its layout and usage, and no damage was reported. Geometric data were checked. Laboratory tests were conducted in order to obtain the data about mechanical and physical properties of materials. Specifically, the brick unit compressive strength, and the compressive strength of concrete walls, were determined.

The compressive strength of bricks and concrete was obtained based on experimental tests made at the Institute for Structures and Materials of the Civil Engineering Faculty in Sarajevo, Bosnia and Herzegovina. This was the starting point for determining input data for numerical modelling. It was established that the compressive strength of bricks corresponds to the class M150 (new M15) and that it fulfils requirements for load-bearing walls. As it was impossible to take mortar samples from the structure, the decision was made to approximate the compressive strength of mortar, and the value of 2.5 N/mm^2 was adopted based on numerous previous investigations conducted by the Institute for Structures and Materials in Sarajevo. Tests conducted on cylindrical concrete specimens (diameter 100 mm) revealed that the concrete grade is MB25, which is roughly equivalent to C20/25 in Eurocode 2, and that the reinforcement is 14 mm in diameter. The steel grade is GA240/360 (with the yield strength of 240 N/mm^2). The location of the specimens is labelled in Figure 5.a and Figure 5.b for the masonry and concrete, respectively.

3.3.1. Material properties

As per equation (1), and with K = 0.45, the compressive strength is f_k = 4.07 N/mm^2. The structure was analyzed with both modulus of elasticity values. According to equation (2), the value amounts to E = 4070 N/mm^2 and, according to equation (3), the modulus of elasticity amounts to E = 3052,5 N/mm^2. However, only the value recommended in Eurocode 6 will be presented in the paper.

The density of this type of masonry amounts to 1900 kg/m^3. However, the value was proportionally increased to take into account the non-bearing façade walls with respect to the mass, while keeping the thickness of d = 25 cm, which enables stiffness to remain intact (shown in Table 1 with *).

The tensile fracture energy can be calculated using the expression (4) G_f = 0.10 N/mm. The compressive fracture energy, as defined in equation (6), is equal to G_{fk} = 6.51 N/mm.

The input data are shown in Table 1.

The values show a good correspondence when compared to mechanical properties of existing buildings, provided in [15] and [16] and indicated in parenthesis.

Table 1. Masonry data used as input data for modelling

Material properties / Element	Compressive Strength f_k [N/mm²]	Compressive fracture energy, G_{fk} [N/mm]	Tensile strength f_t [N/mm²]	Tensile fracture energy, G_f [N/mm]	Shear strength as per EC6 [N/mm²]	Modulus of elasticity, E [N/mm²]	Poisson's ratio ν	Density ρ [kg/m³]
Façade masonry walls (25+12.5 cm) thick	4.07 (1.5-10)	6.51	0.20 (0.10-0.70)	0.10	1.02	4070 (1500-3800)	0.20	2700*
Inner masonry walls 25 cm thick	4.07 (1.5-10)	6.51	0,20 (0.10-0.70)	0.10	1.02	4070 (1500-3800)	0.20	1900

Table 2. Concrete data used as input data for modelling

Material properties / Element	Mean compressive strength, f_{cm} [N/mm²]	Mean tensile strength, f_{ctm} [N/mm²]	Modulus of elasticity, E [N/mm²]	Poisson's ratio ν	Density ρ [kg/m³]
Floors 26.5 cm thick	24	2.2	27000	0.20	2190
Roof 43.5 cm thick	24	2.2	27000	0.20	2050
Concrete walls 38, 30 and 25 cm thick	24	2.2	30000	0.20	2400

As per experimental testing, it was determined that the equivalent class for MB25 is roughly C20/25, and so mean values from Eurocode2 [17] are adopted in calculation and presented in Table 2.

3.3.2. Non-linear behaviour

The physical non-linear behaviour of the masonry walls is defined by adopting the total strain fixed crack model, as detailed in DIANA [18]. A parabolic stress-strain relation for compression, based on the Hill-type yield criterion, was chosen for nonlinear behaviour of masonry, with no lateral confinement and no lateral crack reduction, having the compressive strength of f_k= 4.07 N/mm², and the corresponding compressive fracture energy of G_{fk}= 6.51 N/mm. The tension path, based on the Rankine-type yield criterion, was described via the exponential tension-softening diagram with the tensile strength of f_t = 0.2 N/mm² and the tensile fracture energy of G_f = 0.1 N/mm. The post-cracking shear behaviour was defined by taking into account the retention factor of its linear behaviour, i.e. the shear retention factor, β = 0.01 [18]. Additional details are provided in [18, 11-13]. This material nonlinearity is presented in Figure 3. The Rayleigh damping was chosen as the building has a similar structural system and structural material throughout its height. The same iteration method (Newton-Raphson) was used for the Pushover and Time History Analysis (THA), while an implicit Hilbert-Hughes-Taylor method [18] had to be used for time integration. The reasoning behind this lies in the fact that masonry has a very low tensile strength and, thus, there is a rapid transition from the elastic range to the fully cracked stage, with development of a large number of distributed cracks, leading to almost no stiffness.

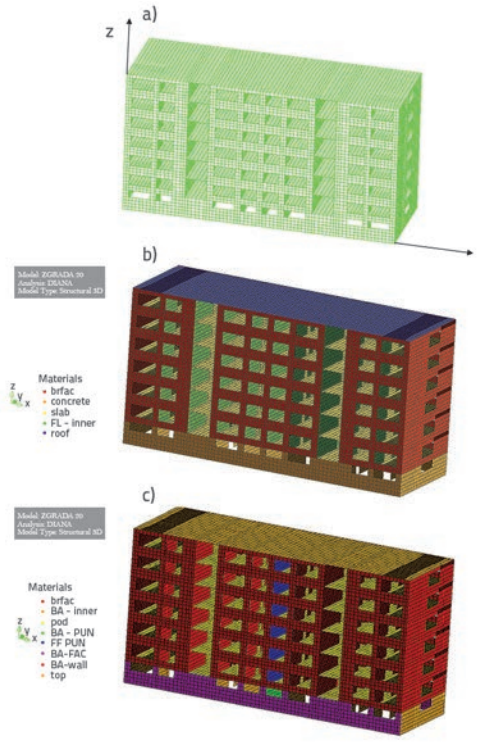

Figure 6. a) final 3D numerical model; b) various material properties; c) various physical properties

3.3.3 Structural Model

The structure was modelled by means of the Finite Element Method (FEM), using curved shell elements corresponding to the quadrilateral element. This kind of element is characterized by 8 nodes and 5

degrees of freedom for each node (40 DOF per element). After meshing, the final 3D numerical model consists of 84523 nodes and 28522 elements, cf. Figure 6.a. Various material and physical properties are presented in Figure 6.b and Figure 6.c, respectively.

The in-plane Gauss integration scheme with 3x3 integration points on the sides, which is a minimum according to Zienkiewicz [19], was selected for the chosen quadrilateral elements. In order to capture the non-linear behaviour, 5 points were selected throughout the thickness, as defined by the Simpson rule. The Regular Newton-Raphson method was chosen as the iteration method.

The Linear Static Analysis and Modal Analysis were conducted for the entire structure. The real stiffness of elements was taken into account. The calculation showed that the floors are rigid, thus enabling distribution of lateral loads to the walls, due to their stiffness. The mesh was kept the same for the Static Non-Linear Analysis (Pushover), and Dynamic Time History Analysis. However, as the structure is symmetric, only a half of the structure was analyzed and appropriate constrains were applied. Thus, one half of the structure was modelled with 45443 nodes and 15759 elements. Regarding the THA, the structure was exposed to Petrovac earthquake as scaled to different accelerations, namely 0.1 g, 0.2 g and 0.43 g.

4. Results

4.1. Linear static analysis

The linear static analysis was conducted to check the reactions, stresses, strains, displacements due to self weight of the structure, and the structure's overall behaviour. As indicated in Section 3, the floors were modelled as linear elastic elements, and the analysis was made to check whether principal stresses in the floors are lower than the tensile strength. As can be seen in Figure 7, the major part of the slab has the tensile stress of less than 2.2 MPa, with few peaks at the locations of the walls, which is due to the compatibility conditions.

4.2. Pushover analysis

The non-linear static analysis (pushover analysis), a performance-based methodology relying on an incremental increase of a pre-defined horizontal force distribution, was applied on the structure having constant gravity loads. The structure was exposed only to the horizontal forces in the "± Y" direction, and the displacement of the point at the top of the building was observed and labelled as 44014 (Figure 8). The horizontal load was applied in a stepwise fashion, proportional to its mass. The capacity curves were obtained by connecting the load factor (coefficient) and the horizontal displacement using the following formulation (7):

$$\alpha = \frac{\sum F_H}{\sum F_V} \cdot 100 \ [\%] \tag{7}$$

where:

$\sum F_H$ - is the total sum of reactions at the base of the structure (base shear), and

$\sum F_V$ - is the total sum of reactions at the base of the structure due to vertical loads (gravity load).

The control node 44014 was chosen in the line of symmetry at the roof level, as shown in Figure 8, and two additional nodes (nodes 44035 and 43935) were selected in the same line in order to examine the slab behaviour.

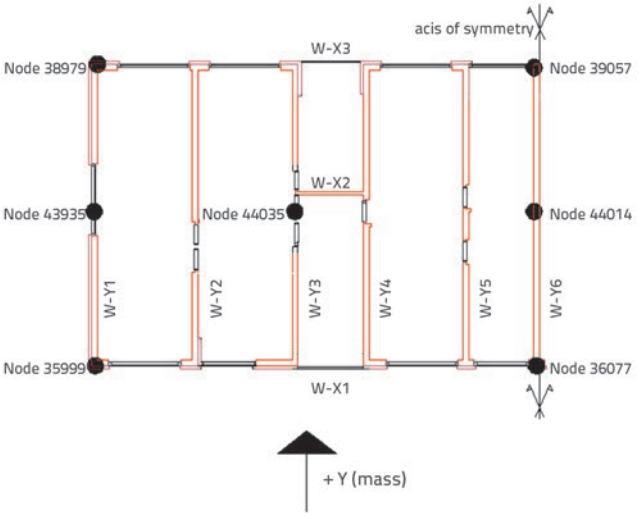

Figure 8. Location of nodes, wall labelling, and direction of horizontal force

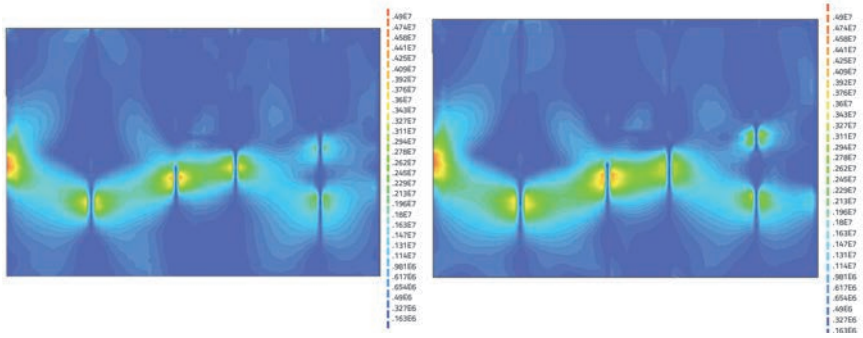

Figure 7. Tensile stresses in slabs of 1st and 2nd floors, at the final stage

Node movements at the top of the structure along the same horizontal line (43935, 44035 and 44014), as shown in Figure 9, were investigated in order to prove the rigid-floors assumption. As illustrated in Figure 11, the movements of these nodes were the same, which shows that the slab behaviour is rigid.

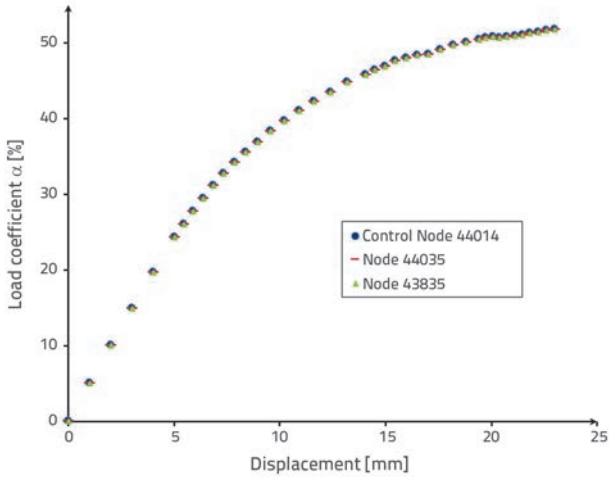

Figure 9. Capacity curves for nodes 44014, 44035, and 43935

4.2.1. Pushover - development of the cracks

In order to comprehend the non-linear behaviour of the structure, three points characteristic for nonlinear behaviour, corresponding to load coefficients α = (24.3; 39.7; 51.8 %), were selected on the capacity curve, see Figure 9. Then, the principal tensile strains at these stages were analyzed for the transverse load bearing walls and façade bearing walls.

The first stage corresponds to the load coefficient of α = 24.3 % (starting of the visible non-linear behaviour), the second to α = 39.7 %, and the third stage (being the final one) to α = 51.8 %. The stages are almost at the same distances, and so the damage pattern can properly be followed.

As can be seen in Figure 10, the formation of the cracks starts at the load bearing walls (parallel to the action of the force-Y direction). The first cracks form around the openings, which is due to concentration of stresses and "weak" points in the structure. The first cracks at the façade walls (X direction) appear at the upper floors, and then the cracks appear on the ground level at the wall W-X1. The cracks are then observed at the load bearing wall W-Y1, and then continue to the load-bearing walls W-Y3 and W-Y4. The behaviour of the structure is governed by the walls in Y direction.

However, at the 2nd stage, with the load coefficient of α = 39.7 %, a large number of new cracks appear and their propagation is seen on the wall W-Y6. From this moment onward, the cracking becomes more visible in the walls W-Y5, W-Y4, continuing with walls W-Y1, whereas the five times smaller amount of cracks appears in the walls W-Y2 and W-Y3. This is evidently related to the individual stiffness of the walls, and there is an obvious redistribution of the stresses. The redistribution of seismic loads is possible due to the available ductility of the walls, which enables redistribution of seismic loads from the most damaged walls to the less damaged ones, and even to the undamaged wall. In this way, the energy is being dissipated during the seismic response of the building.

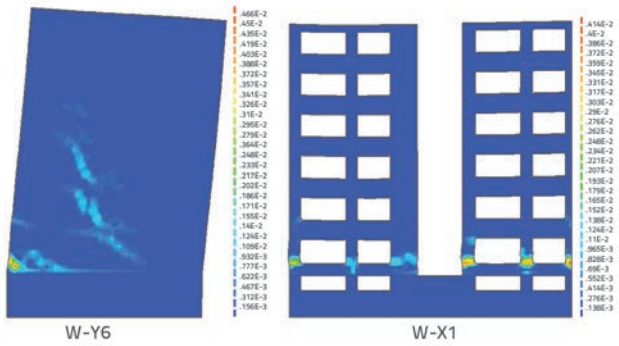

Figure 11. Principal tensile strains of load bearing walls W-Y6 and façade wall W-X1 (α = 39,73 %)

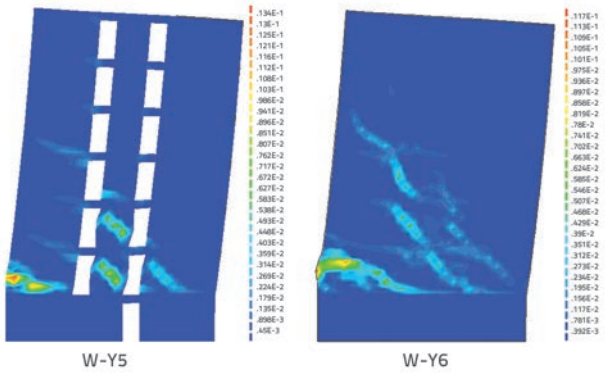

Figure 12. Principal tensile strains of load bearing walls W-Y5 and W-Y6 (α = 51,8 %)

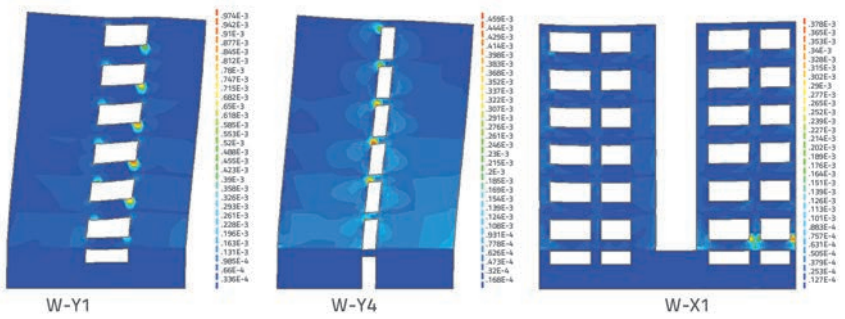

Figure 10. Principal tensile strains of load bearing walls W-Y1, W-Y4 and façade wall W-X1 (α = 24,3 %)

The crack concentration can be observed in the façade wall (W-X1) at the ground floor level. The formation of cracks at the corner of longitudinal and transverse walls, and at the location of the openings, is more than evident (Figure 11).

Major cracks occur at the level between the basement walls and the ground floor. It can be seen that the basement is actually rigid while the upper part of the structure is behaving like an "another" body having its own movements. This

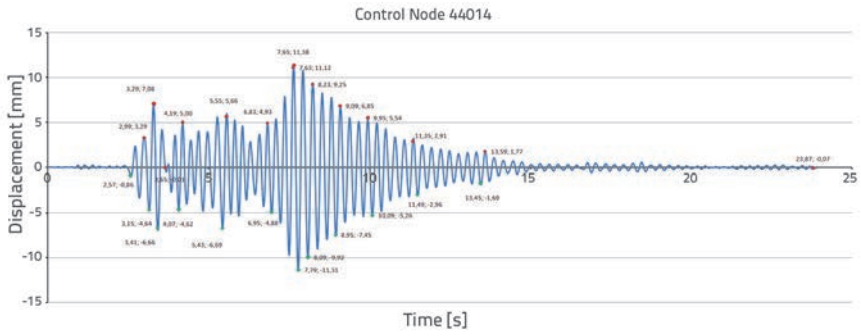

Figure 13. Horizontal displacement of control node 44014 as related to time

kind of behaviour can be explained by a large difference in stiffness between the basement walls made of concrete, and the upper walls made of masonry. Finally, at the 3rd stage α = 51.83 %, the largest amount of cracks is located at the walls W-Y6 and W-Y5, and is caused by shear (Figure 12).

4.2.2. Time history analysis - development of cracks

a) a_g = 0.1 g

In order to view the development of damage to the structure during an earthquake, it was necessary to investigate the damage pattern (principal tensile strain distribution) in different time steps. The displacement vs. time of the Control Node 44014 (as in the pushover analysis) was chosen and plotted as shown in Figure 13. The maximum displacement amounts to -11.38 mm at the time of 7.65 s.

It is interesting to consider plastic or permanent deformations. First plastic deformations appeared at the time t = 3.29 s (permanent damage), and were observed at the façade longitudinal walls (W-X1 and W-X3) on the upper levels around the openings. At the same time, smaller damage was seen on the transverse wall (W-Y1) under the window located on the top floor, as shown in Figure 14.

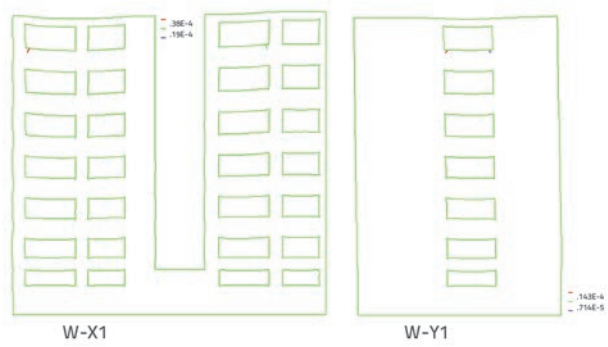

Figure 14. Permanent damage observed at time t=3.29s

The development of shear cracks (elastic and plastic) after 7.79 s is shown in Figure 15 (left-hand side), while only permanent cracks are shown at the right-hand side of the same figure. It is clear that the damage is concentrated at the lower floors of the structure, as well as in the areas around the openings. Cracks clearly reveal a diagonal formation pattern, which is typical for this type of structures due to horizontal forces. Vertical cracks appear in the areas around the openings, which is due to bending. Horizontal cracks are seen in the upper levels, mainly locally, and this can be attributed to the local pure shear due to low vertical load.

An irreversible crack propagation on a half of the structure is shown in Figure 16 where the largest concentration of cracks can be seen in the walls W-Y6 and W-Y4, while the widest cracks are observed at the ground level of the longitudinal façade wall W-X1, as well as at the wall W-X3. Local and wider cracks are also located at the transverse walls near the openings where the concentration of stresses is seen from the beginning of the earthquake action. The redistribution of stresses is observed, i.e. the transfer from the locations suffering greatest damage to the less damaged elements. The final plastic damage after termination of the earthquake action is shown in Figure 17.

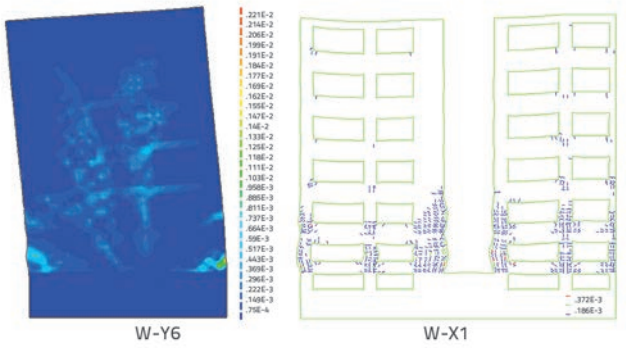

Figure 15. Damage of walls W-Y6 and W-X1 (7.79 s)

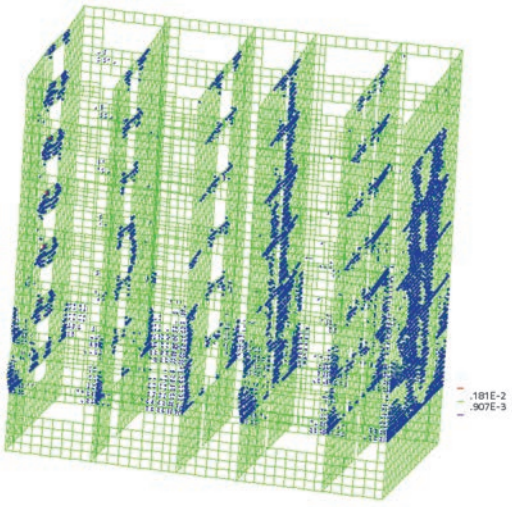

Figure 16. Propagation of permanent cracks on the entire structure at 7.79 s of the earthquake

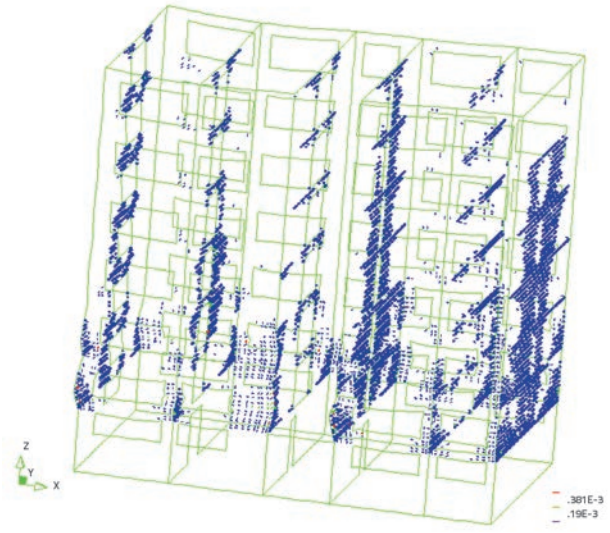

Figure 17. Crack propagation on the entire structure at the end of the earthquake (0.10 g)

Regarding the global behaviour of the structure examined in this case study, it can generally be correlated with experimental investigations conducted by Tomaževič in 1991 [15], where the study of a similar building revealed that there is a concentration of damage in the first floor, as illustrated in Figure 18.

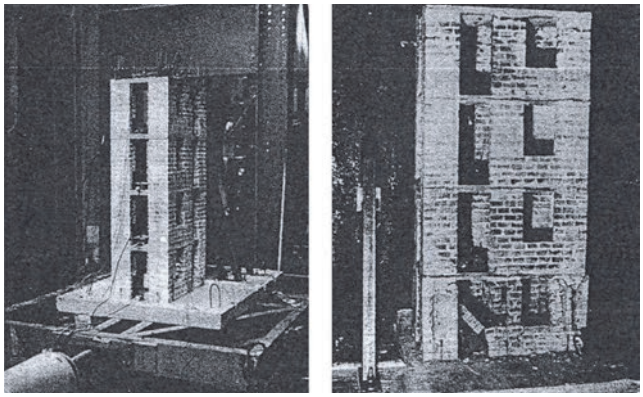

Figure 18. Experiments for a 4-storey masonry building [15]

In this case, the ground floor can be regarded as the first floor due to high stiffness of the basement made of reinforced concrete. This indicates that this type of masonry structures can be modelled as a storey mechanism mode - shear wall with pier action [15, 20]. The basic assumptions of this model are: good connection between the walls, with floors that can be considered as axially stiff in their plane. This means that seismic forces are transferred to the walls due to their stiffness, and this hypothesis was also used in the modelling procedure. Accordingly, a good correlation between this experimental testing and the structural model was established.

b) a_g = 0.2 g

Additionally, the analysis of the structure was conducted for the same earthquake action equivalent to the ground acceleration of a_g = 0.2 g. Time-related displacement of the control node 44014 is shown in Figure 19.

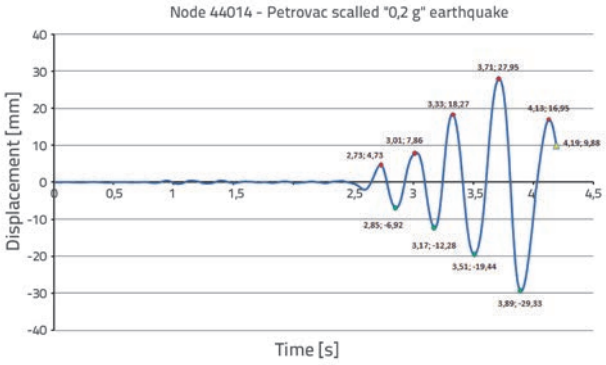

Figure 19. Horizontal displacement of control node 44014

The structure was highly damaged after t = 4.19 s, and the calculation was stopped. The evolution of permanent cracks at t = 3.71 s is illustrated in Figure 20. Here, the maximum displacement at the top of the structure (control node 44014) amounts to approximately 30 mm. The damage concentration is also evident at lower levels of the structure, with a gradual propagation towards the upper floors.

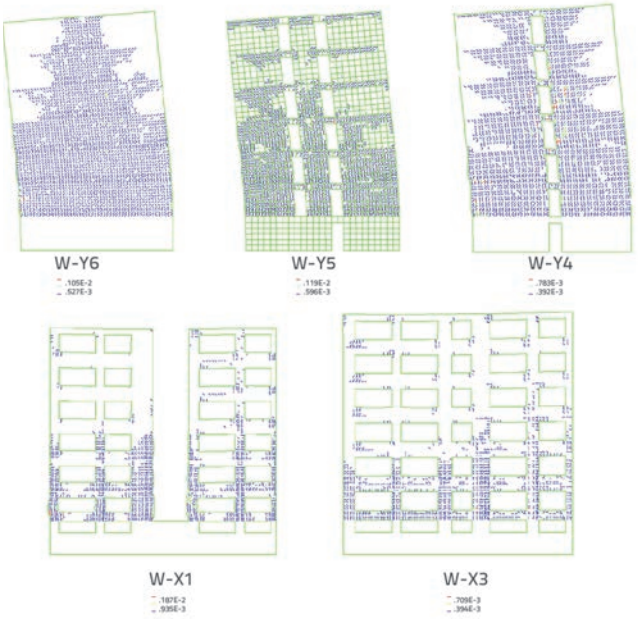

Figure 20. Permanent cracks at t=3.71s

c) a_g = 0.43 g

When the structure is exposed to the real Petrovac earthquake, which occurred in 1979, with the maximum ground acceleration of a_g = 0.43 g, the damage to the structure is evident already at t = 3.65 s, and the structure collapsed as shown in Figure 21.

In that respect, Figure 22 shows damage to the structure and its collapse at the level between the basement and the ground

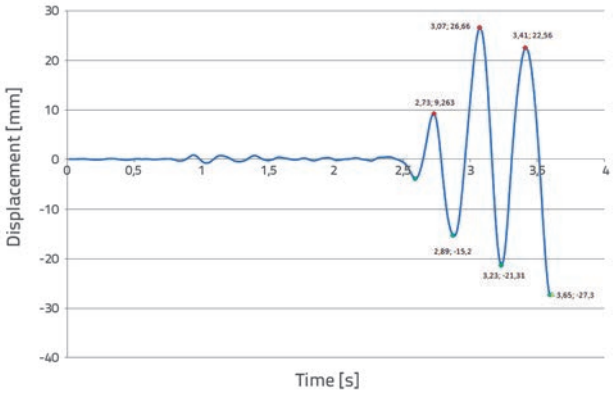

Figure 21. Horizontal displacement of control node 44014

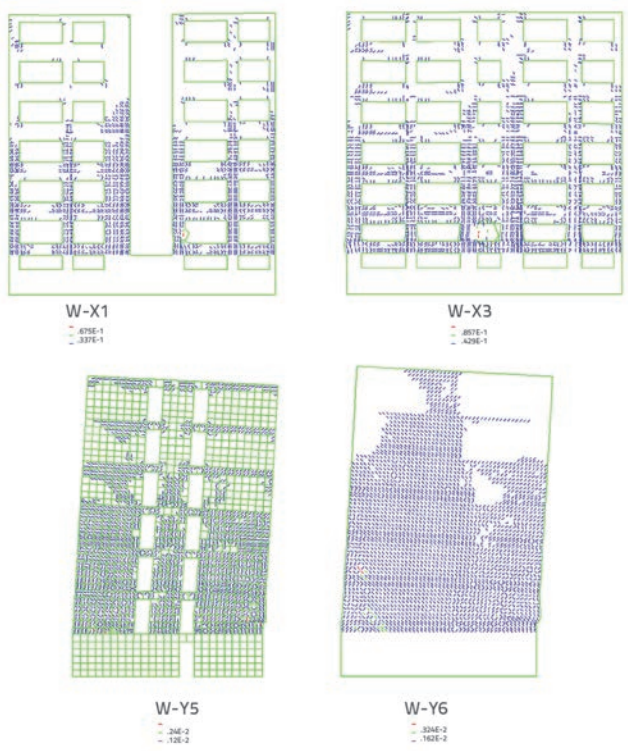

Figure 22. Failure of structure

floor due to a remarkable change in stiffness. The observed damage and collapse can be related to the building illustrated in Figure 1 after the Skopje earthquake. It is evident that this type of structures, typical for the entire region, is unable to withstand an earthquake of such a high ground acceleration.

Parts of hysteresis curves for all three cases, and the capacity curve for the pushover analysis, are shown in Figure 23. As can

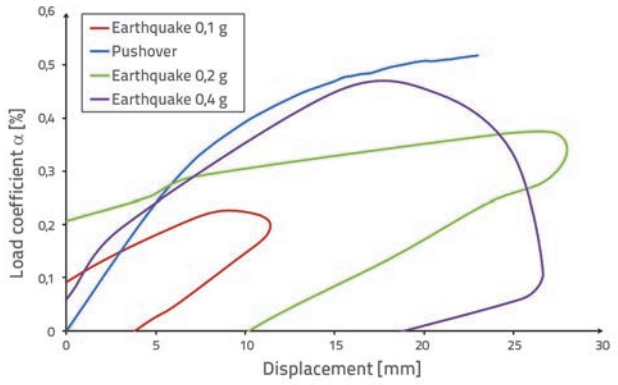

Figure 23. Parts of hysteresis curves and capacity curve

be seen, relatively small displacements can be observed for the structure subjected to the earthquake action of a_g = 0.10 g. It is evident that the significant damage and energy dissipation can be observed when the ground acceleration equals a_g = 0.20 g, while the entire capacity of the structure is exhausted for the real Petrovac earthquake. It is important to mention that an unacceptable inter-story drift amounting to 5.77 % was observed during the earthquake action with the ground acceleration of a_g = 0.20 g, and so the building can not be considered safe for this earthquake action [11, 12].

5. Conclusion

The results obtained show that the structure is characterized by typical shear behaviour. The walls parallel to the load exhibit diagonal cracking caused by horizontal forces, as well as the diagonal "X" type cracking due to cyclic loading. The concentration of damage at the location of the openings is due to the concentration of stresses. The earthquake action causes major damage to the load-bearing walls that are governing the behaviour of the structure. This can be seen at lower levels of transversal walls (Y direction). The damage is concentrated between the basement and the ground floor, which can be explained by the discontinuity and large difference in stiffness. Major damage was registered at lower floors where the largest inter-story drift, with severe deformation and ductility in lower floor zones, was observed. This kind of behaviour was identified in previous earthquakes on a similar structure in Skopje, and by experiments conducted by Tomaževič in Slovenia. The damage slowly propagates to the upper floors on the façade walls. The earthquake action causes degradation of stiffness in the multi-storey masonry structure.

REFERENCES

[1] Hrasnica, M.: *Seizmička analiza zgrada*, Gradjevinski fakultet Sarajevo, 2005 (in Bosnian).

[2] Hrasnica, M.: Damage assessment of masonry and historical buildings in Bosnia and Herzegovina, Damage assessment and reconstruction after war or natural disasters, eds. Ibrahimbegović, Zlatar, Springer Verlag, pp. 333–56, 2009., doi: http://dx.doi.org/10.1007/978-90-481-2386-5_13

[3] Petrovski, T. Jakim: Damaging Effects of July 26, 1963 Skopje Earthquake, *International Conference 40 years 1963 Skopje Earthquake*, European Earthquake Engineering (SE-40EEE), pp.1-16, 2003.

[4] *European macro seismic scale 1998*, EMS-98, Vol.15. Luxemburg: Center Europèen de Gèodynamique et de Séismologie, (ed. Grunthal, G.) pp. 1–101, 1998.

[5] Rots, J.G.: Numerical simulation of cracking in structural masonry, *Heron*, 36(2), pp. 49-63, 1991.

[6] Eurocode 6: Design of masonry structures. Part 1–1: General rules for reinforced and unreinforced masonry structures. European Pre-standard ENV 1998. Bruxelles: Comite Europeen de Normalisation; 2002; 1996.

[7] Paulay, T., Priestley, M.J.N.: *Seismic Design of Reinforced Concrete and Masonry Buildings*, John Wiley & Sons, Inc.1997.

[8] Lourenço, P.B., Barros, J.O., Oliveira, J.T.: Shear testing of stack bonded masonry, C*onstruction and Building Materials*, Vol. 18, pp.125-132, 2004., doi: http://dx.doi.org/10.1016/j.conbuildmat.2003.08.018

[9] Model Code 90CEB-FIP: Comité Euro-International du Béton d'Information Lausanne, Thomas Telford Services, 1993.

[10] Lourenço, P.B.: *Recent Advances in Masonry Modeling: Micro-Modeling and Homogenization* (Chapter), *Multiscale Modeling in Solid Mechanics: Computational Approaches*, eds. U. Galvanetto & M. H. Aliabadi, Imperial College Press, London, pp. 251-294, 2010.

[11] Ademović, N.: Structural and seismic behavior of typical masonry buildings from Bosnia and Herzegovina, MSc thesis. University of Minho, 2011.

[12] Ademović, N.: Ponašanje zidanih konstrukcija u BiH pri dejstvu zemljotresa sa stanovišta savremenih teoretskih i eksperimentalnih saznanja, doktorska disertacija, Građevinski fakultet Univerziteta u Sarajevu, 2012 (in Bosnian).

[13] Ademović, N., Hrasnica, M., Oliveira, D.V.: Pushover analysis and failure pattern of a typical masonry residential building in Bosnia and Herzegovina, *Engineering Structures*, Vol. 50, pp.13-29, 2013., doi: http://dx.doi.org/10.1016/j.engstruct.2012.11.031

[14] Mendes, N. Lourenço, P.B.: Seismic assessment of masonry ''Gaioleiro'' building in Lisbon, Portugal. *Journal of Earthquake Engineering*, 14(1), pp. 80–101, 2010.

[15] Tomaževič, M.: *Earthquake-resistant design of masonry buildings. Tom. I.*, Imperial College Press, 1999., doi: http://dx.doi.org/10.1142/p055

[16] Sorić, Z.: *Zidane konstrukcije, drugo izdanje*, Hrvatski savez građevinskih inženjera, Zagreb, 2004.

[17] Eurocode 2: Design of concrete structures. Bruxelles: Comite Europeen de Normalisation; 2002.

[18] DIANA 9.4. TNO.: Displacement method ANAlyser 9.4. Finite element analysis. User's manual, release 9.4. Netherlands, 2009.

[19] Zienkiewicz, O.C., Taylor, R.L., Zhu, J.Z.: *The finite element method: its basis and fundamentals*. Elsevier, 2005.

[20] Tomaževič, M.: Dynamic Modeling of Masonry Buildings: Storey Mechanism Model as a Simple Alternative, *Earthquake Engineering and Structural Dynamics*, Vol. 15, pp. 731-749, 1987., doi: http://dx.doi.org/10.1002/eqe.4290150606

[21] Eurocode 8: Design of Structures for Earthquake Resistance, Part 1: General rules, seismic action, and rules for buildings, Brussels, 2004.